Early Thermographic Screening of Breast Abnormality in Women with Dense Breast by Thermal, Fractal, and Statistical analysis

Deepika Singh (rse2018507@iiita.ac.in)
Indian Institute of Information Technology Allahabad https://orcid.org/0000-0001-8280-6574
Ashutosh Kumar Singh
Indian Institute of Information Technology Allahabad
Sonia Tiwari
Kamala Nehru Memorial Hospital: Kamala Nehru Memorial Hospital and Regional Cancer Centre

Research Article

Keywords: Breast cancer, breast thermogram, early screening, dense breast, statistical features, fractal dimension, and hot-spot

Posted Date: April 7th, 2022

DOI: https://doi.org/10.21203/rs.3.rs-1442497/v1

Abstract

Objectives: Breast cancer is the prime reason for mortality due to cancer in women across the globe and India. Early screening to identify breast abnormality before the actual symptoms are visible, is the only effective way of reducing associated mortality. Breast thermography, which is a non-invasive, painless, non-toxic, and cost-effective method, can potentially be used for early screening, especially to identify lesions in dense breasts.

Methods: The current study is a single-center preliminary thermography based study of 5 malignant and 7 benign female subjects that highlights the correlation of thermal, statistical, and fractal features obtained from thermograms (malignant and benign), with the clinical characteristics of the patients.

Results: Comparison of mean surface temperatures of 12 subjects shows that the contralateral breast temperature difference is more than 0.5˚C for malignant cases, whereas, for benign cases, the value is between 0 to 0.2˚C. Also, the fractal dimension of the hot spot boundary in the malignant breast side is greater than the corresponding fractal dimension on the contralateral side.

Conclusion: The proposed study is able to identify malignancy in dense breasts cases and benign cases requiring follow-up after screening to reduce the chances of breast cancer progression.

1. Background

Breast cancer [1][2][3] is one of the commonly found cancers in women worldwide. Screening and diagnosis at the initial stage of breast cancer is the only effective way to lower the mortality rate. Breast thermography [4][5][6][7] is a potential adjunct screening tool to existing diagnostic methods like mammography, ultrasonography, magnetic resonance imaging (MRI). This method quantifies the surface temperature of the human body by capturing infra-red radiations emitted by the body surface, using Infrared cameras. The growth of cancerous cells can cause an increase in surface temperature due to pathophysiological changes, i.e. metabolic and vascular changes [8]. Increased metabolic activity results in increased biochemical signaling [9][10]. Change in microvasculature includes the building of new capillary blood vessels (angiogenesis) and vasodilation of blood vessels already present. This can result in a temperature rise [11][12] in cancerous tissue when compared with normal tissue. Existing diagnostic methods like mammography, which is the gold standard technique, have certain limitations like (1) increased chances of cancer with repeated exposure (2) painful method, and (3) not effective for young women having dense breast tissue [13]. MRI is a very effective technique for cancer screening but it is costly and may cause allergic reactions to the patient due to the usage of contrast agents. Clinical breast examination (CBE) is also one of the low-cost key steps in early breast cancer detection when combined with other imaging modalities [14]. Breast thermography is a non-invasive, radiation-free, cost-effective, portable, and contact-less potential screening method for monitoring breast abnormalities. It is suitable for females below 40 years, having dense breast composition. In mammography, sometimes the cancerous growth may be undetected in dense breasts [15]. Moreover, repeated mammogram screening may cause radiation exposure. It is reported that this emerging tool can identify initial signs of cancer 8 to 10 years before mammography[16]. In medicine, this technique has been effectively used for the early identification of inflammatory disease, breast cancer screening, and rheumatology[17]. Breast thermography may prove to be very useful in reaching a large number of people, which may not be having access to advanced diagnostic facilities, especially in developing countries [18][19][20].

Comparison of clinical studies ranging in the period of 1 to 16 years, for and against breast thermography [7][21] show that though many studies showed very high sensitivity (98%) and specificity (99%) with classifiers, this technique is still not used as a standalone breast cancer screening tool due to false positives. However, the tool can potentially be used as an adjunct tool for sequential screening of women to assess chemotherapy response [22]. Most of the recent works related to the analysis of breast thermograms have private databases. The only publically available database is the DMR (Database for Mastology Research) [23]. Another breast thermogram database was created by the Department of Biotechnology-Tripura University-Jadavpur University (DBT-TU-JU) [24] database, using standard acquisition protocols. In addition to using state-of-the-art classifier-based recent research works [25][26] to reduce false positives, integration with oncologists, radiologists, and local health care systems [27] can potentially make thermography a standard tool for screening. The present study is a single-center prospective study performed to achieve the following goals:

- Creation of Breast thermogram database of various breast diseases (including normal, benign, and malignant conditions). These breast thermograms are taken in the last two years from Regional Cancer Centre at Kamla Nehru Memorial Hospital Allahabad. Analysis and diagnosis have been performed at the Indian Institute of Information Technology Allahabad, India. Therefore we have given a name to this database as “KNMH-IIITA Breast thermogram database”.
- Highlight significance of breast thermography in women with dense breasts (malignant and benign) for early cancer screening.
- Correlation of thermal, statistical, and fractal features with clinical findings to reduce false positives
- Identification of benign conditions requiring frequent follow-up.

The main attributes of the KNMH-IIITA Breast thermogram database are enlisted below:

- The database contains breast thermograms of female subjects with normal and various benign (mass of cells that does not invade nearby tissues) and malignant (cells grow uncontrollably and spread to nearby and/or distant body parts) conditions.
- Record of detailed clinical reports, breast density, menopause status, size, and location of the tumor.
- Each subject's thermograms are taken in five different views: frontal, left lateral, right lateral, left oblique and right oblique.
- The database contains 96 thermograms of 12 subjects (5 malignant and 7 benign).
- Out of 5 malignant subjects, we have considered thermograms of 3 malignant cases only, as thermograms of the other 2 subjects were not clear due to the advanced stage of cancer.

2. Methods

The observational single-center study was performed at Kamla Nehru Memorial Hospital and Regional Cancer Centre, Prayagraj, India. In this study, 96 thermograms of 12 female patients in the age group of 25 to 45 years were screened using a thermal camera. Well-defined breast thermogram acquisition protocols [16][24] were strictly followed for capturing images of female subjects. Before the thermography, the subject's informed consent was taken and they were informed that the breast thermogram and the associated data will be utilized only for the academic research. It was made clear that the identity of the subjects, associated data, and images will remain strictly confidential.

The research study was not reviewed by any ethical committee since this is a non-invasive, non-toxic method of breast imaging conducted as a preliminary study to consider the feasibility and application of further such studies. The research was strictly based on the recommendations stated in the Declaration of Helsinki. Informed consent of the female subjects was taken and recorded with strict consideration regarding maintaining the confidentiality of the subject's data and images. Before static thermography, patients were asked to abstain from sunlight, heavy meal, or intense exercises. Images of subjects were taken in a chamber with regulated temperature (which was recorded for reference). Since subjects were mostly from a rural background, they were explained about the importance of timely screening and monitoring of overall and breast health. All the personal details of both malignant and benign female subjects including name, age, sex, blood pressure, weight, menopause status, etc., and details of breast condition (symptoms), if any, and corresponding period, were noted down. Information related to surgeries done before or family history of cancer, if any, was also noted down for comparison.

During the process of taking thermograms, only 1 female person was present along with the oncologists. FLIR E40 thermal camera has been used to acquire breast thermal images, with thermal sensitivity of 0.07 ˚C at 30 ˚C and image resolution of 240 × 320 pixels. The distance of 45.7 cm and 76.2 cm was maintained between the subject and thermal camera, to optimally cover the region of interest, and images were selected based on the patient's framework. FLIR research IR software has been used for transferring and pre-processing acquired breast thermograms. Visible distinguishing features like deformation or nipple inversion were also recorded for correlation. Except for 2 malignant patients with advanced stages of cancer i.e. subject 10 and subject 11, five different views-frontal, left lateral, left oblique, right lateral, right oblique of all subjects were taken.

Wiener filter [28] is applied for noise reduction before segmentation, by producing linear estimation of the original image with minimum mean square error. MATLAB R2020b software is used for post-processing and feature extraction from breast thermograms. Normalization is also done before feature extraction as it helps in monitoring the progression of disease in clinical studies. All other reports of the subjects such as detailed self-examination, CBE, mammography, ultrasonography, MRI, FNAC (Fine needle aspiration cytology), and biopsy, were recorded for comparison. Clinical details of the subjects whose thermograms are taken, along with tumor location and key thermographic observations are given in Table I.

Table I

Clinical Characteristics Of Subjects Along With Tumor Details And Thermograms Findings

Subject	Age	Breast Density	Meno-pause Status	Diagnosis	Breast Side	Histology	Diagnos-tic test for correlati-on	Lesion and Location and type	Thermo-graphic Findings
1	28	normal fibro-glandular	pre	M	right	carcinoma	Mammo, Biopsy	right breast at 2 o'clock position (ill-defined dense lesion of size 39 × 21mm)	hot spot (R)
2	25	-	pre	B	both	fibro-adenoma	USG	many locations in both breasts (Diffusely thickened TDLUs)	no hot spot
3	45	normal glandular	post	M	left	triple-negative infiltrating ductal carcinoma(BIRADS 5)	Mammo, biopsy	left breast at 3 o'clock position(radio-opaque lesion of size 2.2 × 1.9 cm	hot spot in UOQ (L)
4	30	-	pre	B	left	fibro-adenoma	CBE	-	hot spot (L)
5	32	dense breast	pre	B	left	hypertrophied auxiliary tail (BIRADS 3)	MRI	-	Extremely small hot spot (L)
6	45	dense breast	pre	B	right	fibrocystic, cysts in both breasts (R > L)	Mammo FNAC	Tiny cystic lesions	no hot spot
7	37	-	pre	B	left	severe Infection	-	-	hot spot (L, R)
8	37	normal fibro-glandular	pre	B	right	fibro-adenosis	Mammo	-	hot spot(R)
9	29	glandular	pre	B	right	asymmetric breast parenchyma(BIRADS-2)	MRI	-	no hot spot
10	32	predominantly Fatty	pre	M	Right	triple-negative carcinoma(Post chemo and surgery) (BIRADS 2)	MRI	ILQ right breast(post-operative scar, oval circumscribed collection of size 4.7 × 2.0cm)	large hot spot (R)
11	40	heterogeneous Fibro-glandular	pre	M	Left	phylloid Tumor (BIRADS 4)	MRI	All quadrants of the left breast(poorly circumscribed, lobulated lesion of size(5.8 × 6.3 × 6.3cm-AP, TR, CC respectively)	NA
12	25	dense glandular	pre	M	Left	advance cancer, nodal, liver, lung, and bone metastasis (BIRADS 5)	MRI	Multicentrallobulated heterogeneous enhancing mass lesions (L) (one mass of size 3.6 × 4.9 × 3.7 cm in both outer and inner quadrants)	hot spot in UIQ (L) and small hot spot in UIQ (R)

M = malignant, malignant = cells divide without control and spread to other body parts, B = benign, benign remain confined and do not spread to other body parts, BIRADS = breast imaging and reporting data system, BIRADS 2 = 0% likelihood of malignancy, BIRADS 3 = less than 2% likelihood of malignancy, BIRADS 4 = probably malignant with 20 to 35% chances of malignancy mass, BIRADS 5 = highly suspicious of malignancy, UOQ = upper outer quadrant of the breast, Triple-negative = estrogen receptor(ER) negative: progesterone(PR) receptor negative: hormone epidermal growth factor receptor-2(HER-2) negative, ductal carcinoma = cells lining the milk duct in the breast becoming cancerous, mammo = mammography, USG = ultrasonography, CBE = clinical breast examination, MRI = magnetic resonance imaging, FNAC = fine needle aspiration cytology, TDLU = terminal duct lobular units or lobules, AP = anteroposterior view, TR = transverse view, CC = craniocaudal view

Few representative thermograms of the IIITA –KNMH breast thermographic database of some subjects with benign and malignant conditions are shown in Fig. 1.

3. Results

We have performed post-processing of thermograms of subjects to extract and analyze thermal, fractal, and statistical features to identify significant features for distinguishing benign and malignant cases. As the sample size of the present study is very small, we have taken 1 malignant, 1 benign, and 1 normal subject thermogram from the DBT-TU-JU database after requesting access to the database and obtaining permission from authors to use the database for comparison in our analysis.

3.1. Thermal Feature-Based Analysis

After getting the breast thermograms of subjects in five different views under strict acquisition protocol, we have extracted the region of interests i.e. left and right breast regions by manual segmentation. The frontal, oblique or lateral view was selected depending on the presence of a hot spot. Hot spot due to skin overlapping is not considered for analysis. For surface temperature analysis, we have segmented areas with the highest temperature (hot spot) and various other temperature zones. For this, the k-means clustering method [29] is used as it is relatively simple to implement as compared to other segmentation methods. This is an unsupervised centroid-based learning algorithm, where we partition 'n' observation (here pixels) into 'k' clusters so that every observation is a member of the cluster with the nearest mean. After assignment to the closest cluster centroid (center), centroids are recomputed and modified. This process repeats till the centroid converges. Depending on the number of regions to be identified, a cluster number is selected. The highest and second-highest temperature regions are identified and maximum, mean, and lymph node temperatures of both breasts are recorded. This is done by converting segmented regions into corresponding temperature matrices and the difference between contralateral regions temperatures are computed, as shown in Table II.

Table II

Maximum, Mean, And Lymph Node Temperatures of Both Breasts of Patients/Subjects

Subject	Diagnosis	Breast side	View	T_{MAX}		ΔT	T_{MEAN}		ΔT	T_{LYMPH}		ΔT
				L	R		L	R		L	R	
1	**M**	**right**	**oblique**	**36.4**	**37.7**	**1.3**	**36.2**	**37.4**	**1.2**	**37.7**	**-**	**-**
2	B	both	frontal	35.8	36.0	0.2	35.6	35.8	0.2	35.8	35.8	0
3	**M**	**left**	**lateral**	**36.2**	**35.5**	**0.7**	**36.08**	**35.34**	**0.74**	**35.7**	**35.5**	**0.2**
4	B	left	lateral	36.2	36.1	0.1	35.9	35.9	0	36.2	-	-
5	B	left	frontal	36.2	36.0	0.2	35.9	35.9	0	36.2	35.6	0.6
6	B	right	frontal	35.7	35.8	0.1	35.5	35.6	0.1	35.1	35.5	0.4
7	B	left	oblique	36.5	36.3	0.2	36.2	36.1	0.1	36.5	36.8	0.3
8	B	right	oblique	34.3	34.4	0.1	34.1	34.2	0.1	35.1	34.8	0.3
9	B	right	frontal	35.2	35.3	0.1	35.1	35.2	0.1	35.9	36.5	0.6
10	**M**	**right**	**frontal**	**-**	**37.2**	**-**	**37**	**-**	-	-	-	-
11	**M**	**left**	**frontal**	**-**	**36.7**	**-**	**36.5**	**-**	**-**	**-**	**-**	**-**
12	**M**	**left**	**lateral**	**38**	**37.6**	**0.4**	**37.6**	**37.2**	**0.4**	**36.9**	**36.2**	**0.7**
13	B[1]	left	frontal	33.3	33.1	0.2	33.1	33.0	0.1	32.8	32.6	0.2
14	**M**[1]	**left**	**frontal**	**37.4**	**35.4**	**2.0**	**37.1**	**35.1**	**2.0**	**35.6**	**35.4**	**0.2**
15	N[1]	-	frontal	33.8	33.8	0	33.5	33.4	0.1	33.6	33.3	0.3

[1]Subjects 13, 14 and 15 are taken for comparison, from DBT-TU-JU Breast thermographic database [24] with due permission from Author; ΔT = difference between left and right breast temperature (in ˚C), T_{MAX} = maximum surface temperature (in ˚C), T_{LYMPH} = minimum surface temperature at axilla indicating lymph nodes(in ˚C), T_{MEAN} = mean surface temperature (in ˚C), M = malignant, B = benign, N = normal, L = left breast, R = right breast

3.2. Fractal Feature-Based Analysis

Fractal analysis [30][31] plays a significant role in distinguishing a malignant tumor from a benign lesion. A fractal is a non-regular geometric shape that can be further broken into self-identical pieces. Benign lesions have well-defined boundaries whereas malignant masses have irregular boundaries. We have calculated fractal dimension [32][33]by using the power law given as

$$a = \frac{1}{s^D}$$

1

Where *a* denotes self–similar pieces, *s* is the scaling factor, and *D* is the fractal dimension.

We can also write as follows:

$$D = \frac{\log(a)}{\log ? \left(\frac{1}{s}\right)}$$

2

The box-counting method (BCM) has been used to calculate fractal dimension by breaking the image into square regions having the same size and counting the number of boxes that contain the specified part of the image. To detect the edges of segmented warm and hot regions, we have applied canny edge-based detection [34]. Table III shows the fractal dimension of hot spots and warm regions of both malignant and benign subjects for both left and right breasts.

Table III

Fractal Dimension of Hot Spot and Warm Regions of Both Breasts of Patients

Subject	Diagnosis	Breast side	View	Hot Spot		Warm Region		Hot spot
				Boundary		Boundary		
				L	R	L	R	
1	**M**	**right**	**oblique**	**-**	**1.5251**	**1.4132**	**1.3647**	**Present(R)**
2	B	both	lateral	-	-	1.1753	1.1908	None
3	**M**	**left**	**lateral**	**1.1615**	**1.0886**	**1.2445**	**1.2175**	**Present (L)**
4	B	left	lateral	1.1838	-	1.3302	1.1813	Present L)
5	B	left	frontal	-	-	1.2819	1.2207	Present (L)
6	B	right	frontal	-	-	1.3016	1.1814	None
7	**B**	**left**	**oblique**	**1.2438**	**1.232**	1.3716	1.3571	Present (L, R)
8	B	right	oblique	-	0.9861	1.234	1.3387	Present (R)
9	B	right	frontal	-	-	1.0089	1.1615	None
12	**M**	**left**	**lateral**	**1.2571**	**1.1765**	**1.0968**	**0.9482**	**Present(L, R)**
13	B[1]	left	frontal	-	-	1.0715	1.1873	None
14	**M[1]**	**left**	**frontal**	**1.222**	**-**	**1.2827**	**1.1536**	**Present (L)**
15	N[1]	-	frontal	-	-	1.0154	1.15	none

[1]Subjects 13, 14 and 15 are taken for comparison, from DBT-TU-JU Breast thermographic database [16] with due permission from Authors; M = malignant, B = benign, N = normal, L = left breast, R = right breast

3.3. Statistical Feature-Based Analysis

In this study, we intend to extract and identify statistical and texture features [35][36][37] to identify abnormal thermograms from benign thermograms. First-order statistical features like mean, entropy, skewness, kurtosis, variance standard deviation, and maximum intensity, have been directly calculated from the original image intensity values. These features do not contain information about the relationship with neighboring pixels. So, second-order statistical features [38][39] computed from Gray Level Co-occurrence Matrix (GLCM) have also been used to identify features for distinguishing between malignant and benign/normal cases. This is done by computing the difference between statistical and texture features of contralateral breasts in both cases and then comparing mean and standard deviation as seen in Table IV. Since the

sample size for malignant cases in the present study is very small (only 4), we are not able to identify significant features using statistical methods. Table IV and Table V present some of the descriptors of pixel pairs and the key terms computed from GLCM.

Table IV

Mathematical Expression and description of GLCM Texture Parameters [39]

Texture Descriptor	Formula	Significance
Auto-correlation	$?_i?_j(i,j)p(i,j)$	Represents heterogeneity or clustering in an image
Contrast	$?_i?_j\|i-j\|^2p(i,j)$	Represents the special frequency of an image
Correlation	$\sum_i\sum_j \frac{\left(i-\mu_x\right)\left(j-\mu_y\right)p(i,j)}{\sigma_x\sigma_y}$	Represent the linear dependency of pixels on nearby pixels
Dissimilarity	$?_i?_j\|i-j\|.\,p(i,j)$	Represents the distance between pair of pixels
Energy	$?_i?_jp(i,j)^2$	Represents textural uniformity in terms of pixel pair repetition
Entropy	$-?_i?_jp(i,j).\log?(p(i,j))$	Represents degree of disorder between pixels
Homogeneity	$?_i?_j\frac{p(i,j)}{1+\|i-j\|}$	Highlights small gray level difference in pair of pixels
Sum of squares	$\sum_i\sum_j(i-\mu)^2p(i,j)$	Represents deviation from the mean
Sum average	$\overset{2N_g}{\underset{i=2}{?}}ip_{x+y}(i)$	Represents an average of the sum of grey level distribution
Sum variance	$\overset{2N_g}{\underset{i=2}{?}}(i-sumentropy)^2.\,p_{x+y}(i)$	Represents deviation (from the mean) of the sum of grey level distribution
Sum entropy	$-\overset{2N_g}{\underset{i=2}{?}}.\,p_{x+y}(i).\log?(p_{x+y}(i))$	Represents disorder concerning the sum of gray-level distribution
Difference variance	$\overset{N_g-1}{\underset{i=0}{?}}i^2.\,p_{x-y}(i)$	Represents deviation (from the mean) of the difference of grey level distribution
Difference entropy	$-\overset{N_g-1}{\underset{i=0}{?}}.\,p_{x-y}(i).\log?(p_{x-y}(i))$	Represents disorder concerning the difference of gray level distribution
Information measure of correlation 1	$\frac{HXY-HXY1}{\max?(HX,HY)}$	Texture features derived from previously calculated features
Information measure of correlation 2	$\sqrt{(1-\exp[-2(HXY2-HXY)])}$	
Inverse difference normalized	$?_i?_j\frac{p(i,j)}{1+\frac{\|i-j\|^2}{N_g}}$	
Inverse difference moment normalized	$?_i?_j\frac{p(i,j)}{1+\frac{(i-j)^2}{N_g}}$	

Table V Explanation of key terms used to calculate GLCM Texture Parameters [39]

Terms used in Formula	Meaning
N_g	The gray levels in the quantized image
$N_g{}^2$	Size of GLCM
μ	The mean of the whole normalized GLCM
$p_x(i)$	i^{th} term in the marginal probability matrix (MPM) formed by the summation of the rows of $p(i,j)$
$p_y(i)$	i^{th} term in the MPM
μ_x and μ_y	Mean of p_x and p_y respectively
$\sigma_x{}^2$ and $\sigma_y{}^2$	Variance of p_x and p_y respectively
$p_{x+y}(k)$	Contains the terms of probability matrix $p(i,j)$ that corresponds to the summation of a set of pixel pairs
$p_{x-y}(k)$	Contains the terms of probability matrix $p(i,j)$ that corresponds to the difference of a set of pixel pairs
HX, HY, and HXY	Entropy of p_x, p_y and $p(i,j)$ respectively
HXY1	$-\sum_{i=1}^{N_g}\sum_{j=1}^{N_g} p(i,j).\log[(p_x(i).p_y(j)]$
HXY2	$-\sum_{i=1}^{N_g}\sum_{j=1}^{N_g} p_x(i).p_y(j).\log[(p_x(i).p_y(j)]$

Table VI

Mean Difference Between Statistical and Texture Features of Both Breasts of Patients/ Subjects

	Extracted Features	Difference (Mean ± SD)	
		Benign + Normal(8)	**Malignant(4)**
Statistical Features	Mean	21.78 ± 16.88	17.02 ± 11.36
	Entropy	0.3175 ± 0.25	0.3 ± 0.09
	Skewness	0.0125 ± 0.01	0.0125 ± 0.01
	Kurtosis	**0.0017 ± 0.0017**	**0.0027 ± 0.004**
	Variance	**3.0987 ± 3.64**	**8.09 ± 5.73**
	Standard deviation	8.838 ± 4.11	5.09 ± 3.94
	Maximum	11.75 ± 17.76	3.25 ± 2.48
Texture Features	Auto-correlation	1.367 ± 1.36	0.86 ± 0.56
	Contrast	0.033 ± 0.01	0.023 ± 0.01
	Correlation	**0.0101 ± 0.008**	**0.26 ± 0.42**
	Dissimilarity	0.0127 ± 0.01	0.0065 ± 0.0035
	Energy	**0.041 ± 0.03**	**1.688 ± 2.83**
	Entropy	0.125 ± 0.92	0.085 ± 0.05
	Homogeneity	0.0077 ± 0.006	0.005 ± 0.003
	Sum of squares	1.393 ± 1.35	0.87 ± 0.56
	Sum average	0.366 ± 0.29	0.205 ± 0.05
	Sum variance	4.538 ± 4.37	2.175 ± 2.58
	Sum entropy	0.1398 ± 0.0821	0.075 ± 0.04
	Difference variance	0.033 ± 0.01	0.025 ± 0.01
	Difference entropy	0.04 ± 0.03	0.0212 ± 0.01
	Information measure of correlation 1	0.018 ± 0.01	0.0052 ± 0.0028
	Information measure of correlation 2	0.072 ± 0.12	0.013 ± 0.0108
	Inverse difference normalized	0.145 ± 0.03	0.0032 ± 0.0039
	Inverse difference moment normalized	**0.0001 ± 0.003**	**0.00025 ± 0.0004**

4. Discussion

In the current study, thermal analysis is one of the key steps in identifying breast abnormalities in thermograms. According to Freitas, the thermal variation between contralateral areas in a body should be less than 0.5 ˚C. As seen in Table 4.2, we have used the variation in maximum and the mean temperature of contralateral breasts to identify breast abnormalities. We have also recorded differences between lymph node temperatures of both the breasts but these were not used for comparison as 2 subjects had axillary breast tissues seen as hot spots (false positive). For objective analysis based on lymph node temperatures, a larger dataset is required. Comparison of mean temperature values (mean values depend on a large region of pixels thus more reliable) shows that for 3 malignant cases, the difference between contralateral breasts is more than 0.5 i.e. ranging from 1.2˚C to 2˚C. Subject Id-12 has metastasis on both sides so the temperature difference is 0.4˚C. For benign and normal cases, the mean temperature difference is from 0˚C to 0.2˚C. So temperature analysis can indicate the presence of abnormality.

For fractal feature-based analysis, we have identified hot and warm regions of both breasts using k-means clustering. For both hot and warm regions, corresponding boundaries have been computed. Fractal dimensions of whole regions and boundaries of contralateral breasts are compared. From Table 4.3, we observe that for malignant cases, a hot spot is present and the fractal dimension (FD) of the edge of the hot spot in the malignant breast side is greater than FD of the edge of the hot spot on the contralateral side. Correlating this information with cases where the temperature difference is less than 0.5˚C, we can say that hot spot could be due to other factors such as severe infection as in Subject Id-7 or fibro-adenoma (benign breast tumor) as in subject Id-4 (requiring to follow up every 6 months for age below 35). We have also computed the fractal dimension of the boundaries of warm regions of both breasts. This can be used to monitor the chemotherapy response of subjects during sequential screening. The warm region on both breast sides of benign/normal cases could also be due to hormonal changes.

We have computed first-order histogram-based features directly from the original image intensities. We have computed texture features for both malignant and benign/normal cases. After that, the differences between contralateral breast features are calculated to find the mean difference and standard deviation for 8 (benign + normal) subjects and 4 malignant subjects as seen in Table 4.6. We observe that out of 7 statistical features and 17 texture features, kurtosis, variance [41], energy, and correlation features show the greater mean difference in malignant cases as compared to benign/normal cases. Kurtosis represents the shape of the histogram by indicating a peak in the distribution of gray-level within a tumor/lesion. Energy as a texture feature is crucial as it represents texture uniformity and is easy to analyze in terms of visual assessment and computational load. Higher auto-correlation in the benign case may indicate more homogeneity as compared to the malignant case. These features are an important biomarker in identifying tumor heterogeneity. When thermography is applied for monitoring the chemotherapy response, skewness and kurtosis play a significant role in being closely correlated to complete response to therapy [42]. This technique is also suitable for young women with extremely dense breasts, as seen in three of the subjects (Subject Id – 5, 6, and 12) in the current study. Since the sample size for both malignant and benign cases is very small, presently we were not able to identify statistically significant features using the p-value. The authors are in the process of creating a large collection of breast thermograms of normal, benign, and malignant subjects along with metadata based on clinical reports for correlation. We are also performing sequential screening of one of the malignant subjects after various cycles of Neoadjuvant Chemotherapy (NACT) [22] to monitor the treatment response of the specific patient. Current thermography based study has certain limitations like (a) small dataset to draw more conclusive and significant results, (b) thermal abnormalities due to scars, skin lesions, and benign diseases need to be identified based on more significant features, and (c) false positives due to skin overlapping, hormonal changes, and axillary breast tissues, and (d) we have used a thermal camera with the low resolution of 240 × 320 pixels.

5. Conclusion And Futurescope

This study shows the possible application of breast thermography tools for identifying early indications of breast cancer for women with dense breasts, especially in low-income and developing countries where diagnostic facilities are limited. Since the cost associated with this diagnostic tool is very less (except for the initial cost), this tool may potentially become very effective, particularly in developing and low-income countries in the coming years. Also, breast thermography can be potentially used as a supporting technique to existing breast cancer screening and diagnostic methods like mammography, ultrasound, MRI, etc. Since this technique is non-invasive, radiation-free, painless, and portable, it can be easily used in distant and remote areas. We can use initial findings from the current study to develop an integrated thermography-based system for routine screening of asymptomatic and normal female subjects. An abnormal breast thermogram with a relatively high thermal profile can be used to obtain thermal, statistical, and fractal parameters. As we can separate malignant subjects from benign/normal ones using the average temperature difference between left and right breasts, further significant features can be extracted for reliable findings after correlating with reports from other diagnostic methods. False positives can be further eliminated by segmentation of blood vessels using thermograms. The technique is also useful in the follow-up of patients after breast conservation surgery [43]. Due to the current COVID pandemic [44], with the already overburdened Health infrastructure across the globe, there will be increased cases of delayed breast cancer screening, later-stage diagnosis, and worsened prognosis. After conducting this single-center small study based on breast thermography, we understand that the first and foremost step in developing an integrated Computer-Aided Screening and Detection system [31][45] is to collect the static and dynamic (after applying cold stress) breast thermograms of a very large number of both symptomatic and asymptomatic female populations (both urban and

rural). This database needs to be supported by supporting clinical findings and characteristics if any. To perform fast, real-time cost-effective, and accurate monitoring, we need to develop a system with the help of radiologists, oncologists, and local administration.

Abbreviations

MRI Magnetic Resonance Imaging (A medical imaging technique using strong magnetic field and radio waves)

CBE Clinical Breast Examination (Physical breast examination performed by health care professional)

DMR Database for Mastology Research (Online database of thermal, mammographic, and ultrasound images for early breast cancer detection)

DBT-TU-JU Department of Biotechnology-Tripura University-Jadavpur University (Private breast thermographic database)

KNMH-IIITA Kamla Nehru Memorial Hospital- Indian Institute of Information Technology Allahabad (Private breast thermographic database)

FLIR E40 Forward Looking Infra-Red (Thermal camera)

FNAC Fine Needle Aspiration Cytology (Reliable method for screening small breast lesions)

BCM Box Counting Method (Method for calculating fractal dimension)

GLCM Gray Level Co-occurrence Matrix (Matrix containing probability of occurrence of pairs of pixels in an image)

FD Fractal Dimension (Measure of complication of self-similar figure)

NACT Neo-Adjuvant Chemo Therapy (Chemotherapy treatment given to reduce tumor before surgery)

COVID Corona Virus Disease (Current pandemic across the globe)

Declarations

Competing interests: The authors declare no competing interests.

References

1. "'Cancer Figures.'" [Online]. Available: https://www.wcrf.org/dietandcancer/cancer-trends/breast-cancer-statistics. [Accessed: 13-Jun-2020].
2. "Breast Cancer Facts and Figures 2019-2020." [Online]. Available: https://www.cancer.org/content/dam/cancer-org/research/cancer-facts-and-statistics/breast-cancer-facts-and-figures/breast-cancer-facts-and-figures-2019-2020.pdf. [Accessed: 19-Oct-2020].
3. "Breast cancer statistics in India." [Online]. Available: https://gallery-repo.inshorts.com/gallery/view/796e2a89-eb11-4165-90b7-43bbca6c3738. [Accessed: 19-Oct-2020].
4. T. B. Borchartt, A. Conci, R. C. F. Lima, R. Resmini, and A. Sanchez, "Breast thermography from an image processing viewpoint: A survey," Signal Processing, vol. 93, no. 10, pp. 2785–2803, 2013.
5. S. T. Kakileti, G. Manjunath, H. Madhu, and H. V. Ramprakash, "Advances in Breast Thermography," New Perspect. Breast Imaging, 2017.
6. D. Singh and A. K. Singh, "Role of image thermography in early breast cancer detection- Past, present and future," Comput. Methods Programs Biomed., vol. 183, 2020.
7. A. Lozano and F. Hassanipour, "Infrared imaging for breast cancer detection: An objective review of foundational studies and its proper role in breast cancer screening," Infrared Phys. Technol., vol. 97, no. December 2018, pp. 244–257, 2019.
8. A. L. Iii, J. C. Hayes, L. M. Compton, and F. Hassanipour, "Pilot Clinical Study Investigating the Thermal Physiology of Breast Cancer via High-Resolution Infrared Imaging," pp. 1–12, 2021.
9. D. Hanahan and R. A. Weinberg, "Hallmarks of cancer: The next generation," Cell, vol. 144, no. 5, pp. 646–674, 2011.
10. R. J. De Berardinis and N. S. Chandel, "Fundamentals of cancer metabolism," Sci. Adv., vol. 2, no. 5, 2016.
11. H. H. Pennes, "Analysis of Tissue and Arterial Blood Temperatures in the Resting Human Forearm," 1948.
12. R. LAWSON, "Implications of surface temperatures in the diagnosis of breast cancer," Can. Med. Assoc. J., vol. 75, no. 4, pp. 309–311, Aug. 1956.
13. S. H. Heywang-Köbrunner, A. Hacker, and S. Sedlacek, "Advantages and disadvantages of mammography screening," Breast Care, vol. 6, no. 3, pp. 199–207, 2011.
14. L. Provencher et al., "Is clinical breast examination important for breast cancer detection?," Curr. Oncol., vol. 23, no. 4, pp. e332–e339, 2016.

15. C. A, B. A, T. M, P. TJ, and M. A, “Contact Thermography as an Effective Tool for Detection of Breast Cancer in Women with Dense Breasts-A Case Report,” J. Breast Cancer Res. Adv., vol. 2, no. 1, pp. 1–4, 2020.
16. E. Y. K. Ng, “A review of thermography as promising non-invasive detection modality for breast tumor,” Int. J. Therm. Sci., vol. 48, no. 5, pp. 849–859, 2009.
17. O. Maillot et al., “Evaluation of acute skin toxicity of breast radiotherapy using thermography: Results of a prospective single-centre trial,” Cancer/Radiotherapie, vol. 22, no. 3, pp. 205–210, 2018.
18. A. Shamseddine, A. Tfayli, S. Temraz, and R. Abou Mrad, “Breast cancer in low- and middle-income countries: An emerging and challenging epidemic,” J. Oncol., vol. 2010, 2010.
19. H. Sung et al., “Global Cancer Statistics 2020: GLOBOCAN Estimates of Incidence and Mortality Worldwide for 36 Cancers in 185 Countries,” CA. Cancer J. Clin., vol. 71, no. 3, pp. 209–249, 2021.
20. International Agency for Research on Cancer, “India Fact Sheet 2020,” Globocan, vol. 361, p. 2, 2020.
21. S. Bhattacharyya, P. Dutta, and S. Chakraborty, Hybrid soft computing approaches: Research and applications, vol. 611, no. May 2016. 2015.
22. D. Singh, A. K. Singh, and S. Tiwari, “Breast Thermography as an Adjunct Tool to Monitor the Chemotherapy Response in a Triple Negative BIRADS V cancer patient: A Case Study,” IEEE Trans. Med. Imaging, p. 1, 2021.
23. L. F. Silva et al., “A New Database for Breast Research with Infrared Image,” J. Med. Imaging Heal. Informatics, vol. 4, no. 1, pp. 92–100, 2013.
24. M. K. Bhowmik, U. R. Gogoi, G. Majumdar, D. Bhattacharjee, D. Datta, and A. K. Ghosh, “Designing of Ground-Truth-Annotated DBT-TU-JU Breast Thermogram Database Toward Early Abnormality Prediction,” IEEE J. Biomed. Heal. Informatics, vol. 22, no. 4, pp. 1238–1249, 2018.
25. N. I. R. Yassin, S. Omran, E. M. F. El Houby, and H. Allam, “Machine learning techniques for breast cancer computer aided diagnosis using different image modalities: A systematic review,” Comput. Methods Programs Biomed., vol. 156, pp. 25–45, 2018.
26. D. A. Zebari, D. A. Ibrahim, D. Q. Zeebaree, and M. A. Mohammed, “applied sciences Breast Cancer Detection Using Mammogram Images with Improved Multi-Fractal Dimension Approach and Feature Fusion,” 2021.
27. J. A. McDonald et al., “Symposium report: breast cancer in India—trends, environmental exposures and clinical implications,” Cancer Causes Control, vol. 32, no. 6, pp. 567–575, 2021.
28. D. S. khudayer Jadwa, “Wiener Filter based Medical Image De-noising,” Int. J. Sci. Eng. Appl., vol. 7, no. 9, pp. 318–323, 2018.
29. S. Basar, M. Ali, G. Ochoa-Ruiz, M. Zareei, A. Waheed, and A. Adnan, “Unsupervised color image segmentation: A case of RGB histogram based K-means clustering initialization,” PLoS One, vol. 15, no. 10 October, pp. 1–21, 2020.
30. M. EtehadTavakol, C. Lucas, S. Sadri, and E. Ng, “Analysis of Breast Thermography Using Fractal Dimension to Establish Possible Difference between Malignant and Benign Patterns,” J. Healthc. Eng., vol. 1, no. 1, pp. 27–44, 2010.
31. S. H. Wang, K. Muhammad, P. Phillips, Z. Dong, and Y. D. Zhang, “Ductal carcinoma in situ detection in breast thermography by extreme learning machine and combination of statistical measure and fractal dimension,” J. Ambient Intell. Humaniz. Comput., vol. 0, no. 0, pp. 1–11, 2017.
32. K. Harrar and L. Hamami, “The box counting method for evaluate the fractal Dimension in radiographic images,” 6th WSEAS Int. Conf. circuit, Syst. Electron. Control Signal Process., no. 1, p. 385, 2007.
33. J. Wu, X. Jin, S. Mi, and J. Tang, “An effective method to compute the box-counting dimension based on the mathematical definition and intervals,” Results Eng., vol. 6, no. February, p. 100106, 2020.
34. A. Hossam, H. M. Harb, and H. M. Abd El Kader, “Automatic Image Segmentation Method for Breast Cancer Analysis Using Thermography,” JES. J. Eng. Sci., vol. 46, no. 1, pp. 12–32, 2018.
35. E. Y. K. Ng, L. N. Ung, F. C. Ng, and L. S. J. Sim, “Statistical analysis of healthy and malignant breast thermography,” J. Med. Eng. Technol., vol. 25, no. 6, pp. 253–263, 2001.
36. H. Qi, P. Teja Kuruganti, and W. E. Snyder, “Detecting Breast Cancer from Thermal Infrared Images by Assymmetry Analysis,” Med. infrared imaging, pp. 1–22, 2008.
37. S. P. A. Kirubha, M. Anburajan, B. Venkataraman, and M. Menaka, “A case study on asymmetrical texture features comparison of breast thermogram and mammogram in normal and breast cancer subject,” Biocatal. Agric. Biotechnol., vol. 15, pp. 390–401, 2018.
38. N. Aggarwal and R. K. Agrawal, “First and Second Order Statistics Features for Classification of Magnetic Resonance Brain Images,” vol. 2012, no. May, pp. 146–153, 2012.
39. M. Abdel-Nasser, A. Moreno, and D. Puig, “Breast cancer detection in thermal infrared images using representation learning and texture analysis methods,” Electron., vol. 8, no. 1, 2019.
40. R. A. Freitas, J. All, and R. Reserved, Nanomedicine , Volume I : Basic Capabilities Nanomedicine , Volume I : Basic Capabilities, vol. I. 2016.
41. U. R. Gogoi, G. Majumdar, M. K. Bhowmik, A. K. Ghosh, and D. Bhattacharjee, “Breast abnormality detection through statistical feature analysis using infrared thermograms,” 2015 Int. Symp. Adv. Comput. Commun. ISACC 2015, pp. 258–265, 2016.

42. R. D. Chitalia and D. Kontos, “Role of texture analysis in breast MRI as a cancer biomarker: A review,” J. Magn. Reson. Imaging, vol. 49, no. 4, pp. 927–938, Apr. 2019.
43. H. U. Ulmer, M. Brinkmann, and H. J. Frischbier, “Thermography in the follow-up of breast cancer patients after breast-conserving treatment by tumorectomy and radiation therapy,” Cancer, vol. 65, no. 12, pp. 2676–2680, 1990.
44. R. Y. Brzezinski et al., “Automated processing of thermal imaging to detect COVID-19,” Sci. Rep., vol. 11, no. 1, pp. 1–10, 2021.
45. E. A. M. Id, E. A. R. Id, T. G. Id, and O. Karam, “Deep learning model for fully automated breast cancer detection system from thermograms,” pp. 1–20, 2022.

Figures

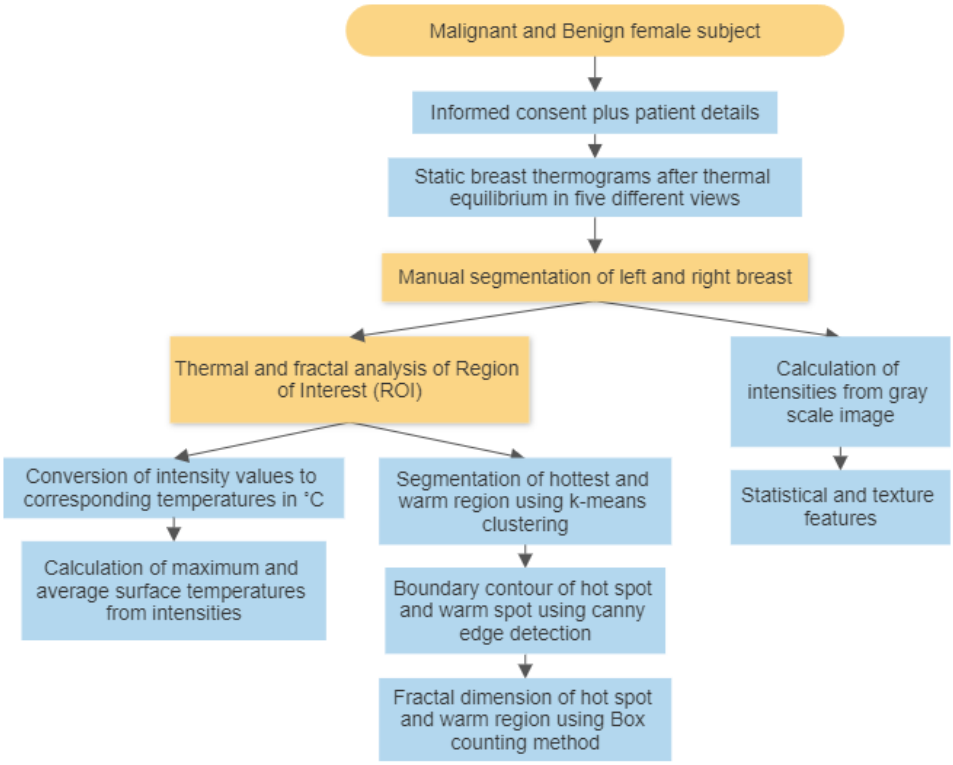

Figure 1

Schematic of breast thermogram analysis of malignant and benign female subjects

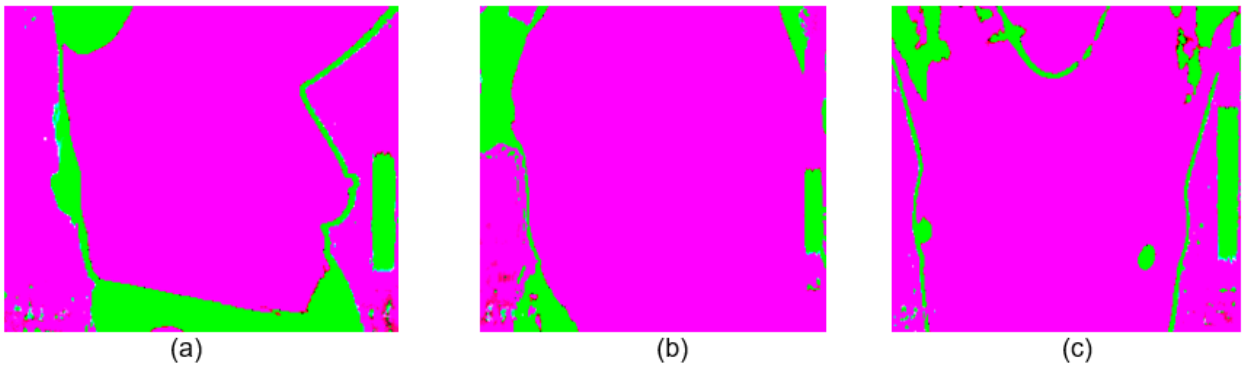

Figure 2

(a) A case of benign disease(Fibroadenosis) in right breast oblique view, with ΔT = 0.1 ˚C, (b) a case of a malignant lesion in right breast oblique view with ΔT = 1.2 ˚C, and (c) a case of proliferative breast cancer in left breast frontal view (metastasis) with ΔT = 0.4 ˚C, ΔT is the average temperature difference between left and right breasts (inframammary fold hot spot is ignored as it is caused by skin folding)